Control of Intramolecular Proton Transfer by a Laser Field

Y. Ohta,* T. Bando, T. Yoshimoto, K. Nishi, H. Nagao, and K. Nishikawa

Department of Computational Science, Faculty of Science, Kanazawa University, Kanazawa 920-1192, Japan

Received: November 14, 2000; In Final Form: May 7, 2001

Intramolecular proton transfer controlled by laser pulses was simulated. The motion of a proton in a molecule was treated by a one-dimensional, asymmetric double-well potential. To control the motion of a proton, a π-pulse approach, stimulated Raman adiabatic passage (STIRAP), and a chirping technique were applied to the system. In the π-pulse approach, the conditions of complete population inversion were determined for sequential and simultaneous irradiation of two laser fields. Similar population dynamics was obtained by a laser pulse sequence designed by global optimal control theory. The results obtained by using STIRAP and the single chirped laser pulse were compared with those obtained by using a π-pulse approach. It was found that a single negatively chirped laser pulse enables fast population transfer but maintains the robustness.

1. Introduction

Recently, much interest has been shown in selective population transfer to a specified quantum state of molecules using a laser field. This is due to developments in laser pulse technology in the past decade. Several approaches based on the coherent interaction of molecules and light have been suggested to prepare a specified state of molecules. For example, the optimal control theory (OCT) presented by Rabitz's group may enable us to design a laser pulse sequence that leads molecules to a desired state.[1−6] By imposing some restrictions on the OCT process, it may be possible to obtain various solutions with desirable properties such as robustness[7,8] and π-pulselike structure. Another example is the generalized π pulse approach presented by Manz's group.[9−17] In their approach, a pulse sequence is made by appropriately optimizing some laser parameters in an analytical function characterizing laser pulse shape. Although this approach enables fast population transfer to a specified state, the pulse sequence requires strict conditions on the laser parameters such as pulse width and intensity to obtain a high product yield. In contrast to the π-pulse approach, the stimulated Raman adiabatic passage (STIRAP) presented by Bergmann's group gives a robust solution. This approach is well-known as an effective technique for population transfer in three-level systems.[18−42] Vibrationally selective population transfer in a ground electronic state of some simple molecules has been experimentally demonstrated,[18−25] and owing to the uniqueness of its pulse sequence, many theoretical studies have been carried out for more than a deade.[26−42] Besides STIRAP, the use of a chirped or swept-frequency laser pulse is also effective for obtaining a robust solution. By using a chirping laser frequency, even a single laser pulse may have many intriguing effects, and thus it has therefore been the subject of many experimental studies[43−50] as well as theoretical studies.[51−61]

Closed-loop learning control is a promising method for controlling a rather complex molecule.[63,64] In this technique, proposed by Rabitz et al., an appropriate pulse sequence is produced by a learning algorithm in which information provided by an experimental device is used as input data. Using this technique, selective bond breaking of a metal complex has been realized.[65]

* Corresponding author. E-mail: yasuto@mcl.chem.tohoku.ac.jp.

As mentioned above, there have been various approaches to the control of chemical reactions. However, to the best of our knowledge, quantum control of an isomerization reaction has not yet been experimentally realized. For the realization of control of such a reaction system, a pulse sequence that has simple structure and can give a robust solution is very attractive.

In the present study, we simulated laser-induced intramolecular proton transfer to control the motion of a proton in a hydrogen-bond system. We treated a substituted malonaldehyde molecule in which the motion of a proton in a molecule is described by a one-dimensional, asymmetric double-well potential. It is thought that this simplified model can describe the essential part of a proton-transfer system well. Thus, the use of this model would enable the dynamical behavior of a proton to be investigated qualitatively, and it would also be a good *server* to find an effective initial trial for a closed-loop laboratory technique. The parameters of the double-well potential are chosen so as to describe substituents such as $-NH_2$ and $-CH_3$.[6] In this model, there is one localized state in each well. We regard one localized state as a reactant and the other as a product. The strategy in our simulations was to induce transition from the reactant to the product by a specific laser pulse sequence. For comparison, we first simulated the control of intramolecular proton transfer by means of the π-pulse approach. In the π-pulse approach, we utilized two sequential and simultaneous laser pulses that have the condition of complete transition from the reactant to the product for an analytical function of laser pulse shape. The pulse sequence was compared with that designed by an OCT process. Next, we simulated the control of proton transfer by STIRAP. The results were compared with those obtained by using the π-pulse approach to show the robustness of STIRAP. The population-transfer process by STIRAP, however, was achieved in about 20 ps, which is longer than that by the π-pulse approach. In this time region, the efficiency of the population transfer may be considerably affected by the relaxation effect resulting from interaction with the environment. To move population more quickly, we utilized a chirped laser pulse. We found that a single negatively chirped laser pulse may enable faster population transfer while maintaining robustness. The robustness of the

10.1021/jp004209a CCC: $20.00
Published on Web 08/04/2001

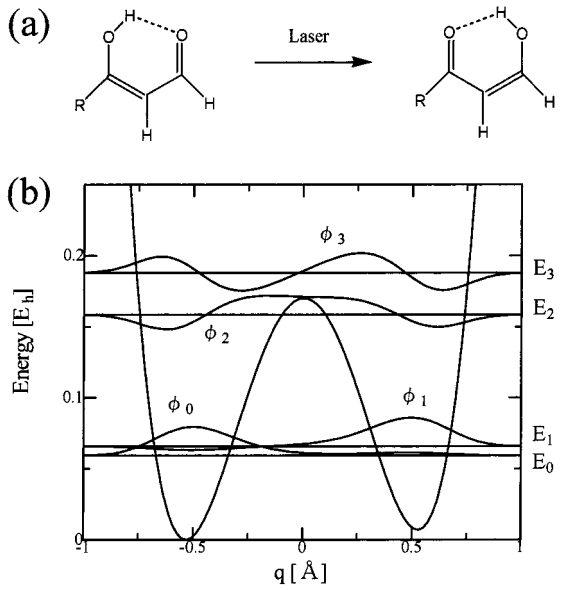

Figure 1. (a) Laser-induced isomerization reaction from the reactant (A) to the product (B) in substituted malonaldehyde. (b) Plot of potential function $V(q)$ for the proton transfer in substituted malonaldehyde: δ is 2.57×10^{-4} E_h, barrier height $V^{\ddagger}$ is 6.25×10^{-4} E_h, and $q_0 = 1.0$ a_0. The lowest four eigenfunctions $\phi_n(q)$ ($n = 0-3$) and associated energy levels E_n are also depicted.

solution was also compared with that obtained by using the π-pulse approach.

2. Model System

As an intramolecular proton-transfer system, we treat substituted malonaldehyde. This molecule may have two stable configurations as shown in Figure 1a. Here, we regard the configuration on the left side in Figure 1 as a reactant and the other configuration as a product. Our strategy is to induce a transition from the reactant to the product by a laser pulse. To simulate laser-induced proton transfer, the proton is assumed to move along a one-dimensional Cartesian reaction coordinate with the limitation that the molecule is in its electronic ground state. Here, we neglect the effect of rotations and coupling to other vibrational modes. The Hamiltonian for the system under consideration is given by

$$H = H_{\mathrm{mol}} + H_{\mathrm{int}} \tag{1}$$

where H_{mol} is the molecular Hamiltonian and H_{int} stands for the interaction of a molecule with the electromagnetic field. The corresponding one-dimensional intramolecular proton-transfer system may be specified as

$$H_{\mathrm{mol}} = -\frac{\hbar^2}{2m_{\mathrm{p}}}\frac{\partial^2}{\partial q^2} + V(q) \tag{2}$$

where m_{p} is the proton mass, q is the Cartesian reaction coordinate, and $V(q)$ is the potential energy. The potential energy $V(q)$ is given by the double minimum potential:

$$V(q) = \frac{\delta}{2q_0} + \frac{V^{\ddagger} - \delta/2}{{q_0}^4}(q - q_0)^2(q + q_0)^2 \tag{3}$$

where δ is the asymmetric parameter and $V^{\ddagger}$ is the barrier height. These values, which are given in Figure 1, were chosen so as to describe the effects of the substituents such as $-CH_3$ and $-NH_3$.[43] The minimum at $q = -q_0 (q_0 = 1.0\ a_0)$ corresponds to the reactant, and that at $q = q_0$ corresponds to the product. H_{mol} satisfies the time-independent Schrödinger equation:

$$H_{\mathrm{mol}}|\phi_n\rangle = E_n|\phi_n\rangle \tag{4}$$

where $|\phi_n\rangle$ is the nuclear eigenstate and E_n the associated eigenenergies. By numerically solving eq 4 using the FGH method,[66] we obtained the nuclear wave functions $\phi_n(q)$. Figure 1b shows the nuclear wave functions together with the potential curve. As seen in Figure 1b, there is one localized state in each well. The reactant corresponds to $|\phi_0\rangle$ localized in the left well, and the product corresponds to $|\phi_1\rangle$ localized in the right well.

We turn to the interaction Hamiltonian H_{int}. This term is semiclassically given by

$$H_{\mathrm{int}} = -\mu \cdot \mathbf{E}(t) \tag{5}$$

where $\boldsymbol{E}(t)$ is the classical electric field and assumed to be linearly polarized to the dominant component of the molecular dipole moment μ. The molecular dipole moment is assumed to be linear for q. For analysis of the dynamical behavior of the system, we expand an arbitrary state $|\Psi(t)\rangle$ in terms of $|\phi_n\rangle$:

$$|\Psi(t)\rangle = \sum_n \exp[-\mathrm{i}E_n t/\hbar] C_n(t)|\phi_n\rangle \tag{6}$$

Substituting eq 6 into the time-dependent Schödinger equation,

$$i\hbar\frac{\partial}{\partial t}|\Psi(t)\rangle = H|\Psi(t)\rangle \tag{7}$$

we have the following differential equation for expansion coefficients of $|\phi_n\rangle$.

$$\mathrm{i}\hbar\frac{\mathrm{d}C_i(t)}{\mathrm{d}t} = -\epsilon(t)\sum_j \mu_{ij} \exp[\mathrm{i}\omega_{ij}t] C_j(t)t \tag{8}$$

where ω_{ij} is the transition frequency:

$$\omega_{ij} = \frac{E_i - E_j}{\hbar} \tag{9}$$

The transition dipole moment μ_{ij} was computed from the wave functions $\phi_n(q)$. The dynamical behavior of the system was investigated by numerically solving eq 8 using the standard Runge−Kutta method. In our simulations, the initial conditions were set to $C_0(t) = 1.0$ and $C_i(0) = 0.0$ ($i \neq 0$) and the lowest 11 eigenstates were used to expand $|\Psi(t)\rangle$ in order to take into account three-photon transition of ω_{30}. We analyzed the dynamics of the system by evaluating the population of each nuclear eigenstate:

$$P_n(t) = |\langle\phi_n|\Psi(t)\rangle|^2 \qquad n = 0, 1, 2, ..., 10 \tag{10}$$

In sections 3 and 4, we applied several kinds of $\epsilon(t)$, which were given by analytical forms or designed by optimal control theory to the proton-transfer system.

3. π Pulse Approaches

In this section, we present the results of simulation of intramolecular proton transfer controlled by π-pulse approaches. To control the motion of a proton, we choose $|\phi_3\rangle$ as an intermediate state due to the strong transition moment for $|\phi_0\rangle$

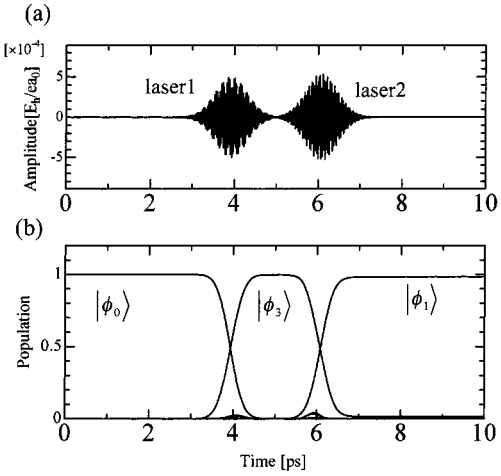

Figure 2. (a) Electric field and (b) population dynamics when two pulses are sequentially applied to the model system of Figure 1. The laser parameters are as follows: $E_1^0 = 5.0 \times 10^{-4}$ E_h/ea_0, $E_2^0 = 5.4 \times 10^{-4}$ E_h/ea_0, $t_2 - t_1 = 2.2$ ps, $\sigma_1 = \sigma_2 = 0.54$ ps, and $\phi = 0$.

and $|\phi_1\rangle$, and we aim to move the population stepwise from $|\phi_0\rangle$ to $|\phi_1\rangle$ via $|\phi_3\rangle$ by using a series of two laser pulses.

$$\epsilon(t) = E_1^0 g_1(t) \cos \omega_1 t + E_2^0 g_2(t) \cos(\omega_2 t + \phi) \quad (11)$$

where E_n^0 and $\omega_n (n = 1, 2)$ are the maximum amplitude and laser frequency of the nth laser pulse, ϕ is the relative phase, and $g_n(t)$ is an envelope given by the Gaussian function with time center t_n and width σ_n:

$$g_n(t) = \exp[-(t - t_n)^2/{\sigma_n}^2] \quad (12)$$

Laser frequencies ω_1 and ω_2 are set to the transition frequencies ω_{30} and ω_{31}, respectively. When there is no temporal overlap between two laser pulses, the process of the population transfer from $|\phi_0\rangle$ to $|\phi_1\rangle$ may be achieved by a sequential inversion of population in two approximate two-level systems composed of $|\phi_0\rangle$ and $|\phi_3\rangle$ connected by laser field 1, and $|\phi_1\rangle$ and $|\phi_3\rangle$ connected by laser field 2. For each two-level system, the condition of complete population transfer[67] is given by

$$\int \mathrm{d}t\, \Omega_{ij}(t) = \pi \quad (13)$$

with

$$\Omega_{ij} = \frac{\mu_{ij} A_n(t)}{\hbar} \quad (14)$$

where $\Omega_{ij}(t)$ is the time-dependent Rabi frequency related to the transition between $|\phi_i\rangle$ and $|\phi_j\rangle$, and $A_n(t)$ is the envelope function of the nth electric field:

$$A_n(t) = E_n^0 \exp[-(t - t_n)^2/{\sigma_n}^2] \quad (15)$$

By substituting eq 15 into eq 13, we can rewrite the condition of complete population transfer as follows:

$$\mu_{ij} E_n^0 = \sigma_n \sqrt{\pi} \quad (16)$$

Figure 2 shows the population transfer from $|\phi_0\rangle$ to $|\phi_1\rangle$ by two sequential π-pulses. The laser parameters are given in Figure 2. Laser1 induces the complete transition from $|\phi_0\rangle$ to $|\phi_3\rangle$, and then laser2 moves the population from $|\phi_3\rangle$ to $|\phi_1\rangle$ to achieve the complete population transfer from $|\phi_0\rangle$ to $|\phi_1\rangle$. The final product yield is 98.3%. The efficiency of population transfer may be considerably influenced by delay time due to other competing processes such as intramolecular vibrational redistribution (IVR). Therefore, to move the population more quickly, we consider the simultaneous irradiation of two laser pulses. To obtain the condition of complete population transfer when two pulses are simultaneously applied to the system, we first expand an arbitrary state $|\Psi(t)\rangle$ in terms of three eigenstates $|\phi_0\rangle$, $|\phi_1\rangle$, and $|\phi_3\rangle$:

$$|\Psi(t)\rangle = \exp[-\mathrm{i}E_0 t/\hbar] C_0(t)|\phi_0\rangle + \exp[-\mathrm{i}E_1 t/\hbar] C_1(t)|\phi_1\rangle + \exp[-\mathrm{i}E_3 t/\hbar] C_3(t)|\phi_3\rangle \quad (17)$$

Substituting eq 17 into eq 7 and making the rotating wave approximation, we obtain the following three differential equations:

$$\mathrm{i}\hbar \frac{\mathrm{d}}{\mathrm{d}t} \begin{pmatrix} C_0(t) \\ C_3(t) \\ C_1(t) \end{pmatrix} = -\frac{\hbar}{2} \begin{bmatrix} 0 & \Omega_{03}(t) & 0 \\ \Omega_{03}(t) & 0 & \Omega_{13}(t) \\ 0 & \Omega_{13}(t) & 0 \end{bmatrix} \begin{bmatrix} C_0(t) \\ C_3(t) \\ C_1(t) \end{bmatrix} \quad (18)$$

The above equations can be easily solved to obtain the analytical form of population $P_1(t)$:

$$P_1(t) = \left(\frac{2\Omega_{03}(t)\, \Omega_{13}(t)}{{\Omega_{03}}^2(t) + {\Omega_{13}}^2(t)} \right)^2 \sin^4 \frac{\sqrt{{\Omega_{03}}^2(t) + {\Omega_{13}}^2(t)}}{4} t \quad (19)$$

From eq 19, the condition of complete population transfer to $|\phi_1\rangle$ is given by

$$\Omega_{03}(t) = \Omega_{13}(t) \quad (20)$$

and

$$\int \mathrm{d}t \frac{\sqrt{{\Omega_{03}}^2(t) + {\Omega_{13}}^2(t)}}{4} = \pi \quad (21)$$

When we employ the Gaussian envelope function (15), eq 20 becomes

$$\frac{E_1^0}{E_2^0} = \frac{\mu_{13}}{\mu_{03}} \quad (22)$$

Figure 3 shows the complete population transfer by the simultaneous irradiation of two laser pulses. The laser parameters are given in Figure 3: The final product yield is 97.5%, and the population transfer is achieved in about 2 ps. We call this pulse sequence a three-level π-pulse. As seen in Figure 3, the laser amplitudes are instantaneously canceled out to produce several nodes due to the interference between two laser fields. In these moments, the time variation of population becomes small because the time-dependent Rabi frequencies instantaneously become zero. The temporal positions of these nodes depend on the relative phase ϕ, although the results are not shown.

4. Laser Pulse Designed by an OCT Process

Next, we present the results of simulation of laser-induced proton transfer by using a pulse sequence designed by a global

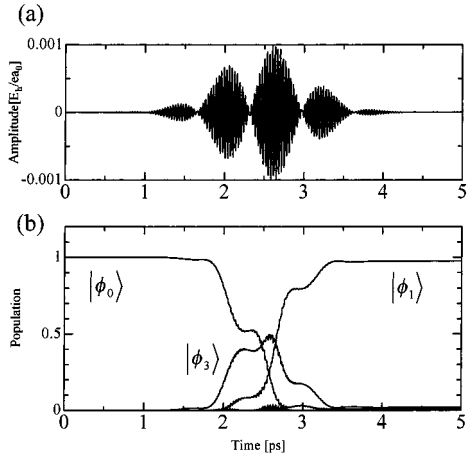

Figure 3. (a) Electric field and (b) population dynamics when two pulses are simultaneously applied to the model system of Figure 1. The laser parameters are as follows: $E_1^0 = 5.0 \times 10^{-4}\ E_h/ea_0$, $E_2^0 = 5.4 \times 10^{-4}\ E_h/ea_0$, $t_2 - t_1 = 0$ ps, $\sigma_1 = \sigma_2 = 0.76$ ps, and $\phi = 0$.

OCT process. In the OCT, $\epsilon(t)$ can be designed by maximizing the following functional:

$$F[\Psi(t),\chi(t),\epsilon(t)] = |\langle\Psi(T)|\phi_1\rangle|^2 - \alpha\int_0^T dt\,\frac{\epsilon^2}{s(t)} - 2Re\left[\langle\Psi(T)|\phi_1\rangle\int_0^T dt\left\langle\chi(t)\left|\frac{\partial}{\partial t} + \frac{i}{\hbar}[H_{mol} - \mu\cdot\epsilon]\right|\Psi(t)\right\rangle\right] \quad (23)$$

where $\Psi(t)$ and $\chi(t)$ are a laser-driven wave function and Lagrange multiplier, respectively. The first term in the right-hand side is the overlap between the laser-driven wave function at the pulse duration time T and the target state $|\phi_1\rangle$. The second term is time-integrated laser intensity, where α is the penalty factor to suppress the laser intensity, and $s(t)$ is the shape function to characterize the pulse envelope of the electric field. In the third term, the boundary condition for $\Psi(t)$ to satisfy the time-dependent Schrödinger equation is imposed. Taking the variation with three arguments $\Psi(t)$, $\chi(t)$, and $\epsilon(t)$ to solve the maximum problem:

$$\delta F[\Psi(t),\chi(t),\epsilon(t)] = 0 \quad (24)$$

we have the following two differential equations with different boundary conditions and the equation for $\epsilon(t)$.

$$i\hbar\frac{\partial}{\partial t}|\Psi(t)\rangle = H|\Psi(t)\rangle \qquad \Psi(0) = \phi_0 \quad (25)$$

$$i\hbar\frac{\partial}{\partial t}|\chi(t)\rangle = H|\chi(t)\rangle \qquad \chi(T) = \phi_1 \quad (26)$$

$$\epsilon(t) = -\frac{s(t)}{\hbar\alpha} Im\langle\Psi(t)|\phi_1\rangle\langle\chi(t)|\mu|\Psi(t)\rangle \quad (27)$$

We numerically solve these three equations in an iterative procedure starting from initial guess $\epsilon_0(t)$ to obtain $\epsilon(t)$, which depends on $\epsilon_0(t)$. As an initial guess, we use two continuous wave (cw) lasers:

$$\epsilon_0(t) = E_1^0 \cos\omega_1 t + E_2^0 \cos\omega_2 t \quad (28)$$

where laser frequencies ω_1 and ω_2 are set to ω_{30} and ω_{31}, respectively, and amplitudes are $E_1^0 = E_2^0 = 3.0 \times 10^{-4}\ E_h/ea_0$. As a shape function, we employ a single Gaussian function with a pulse width $\sigma = 0.76$ ps. The penalty factor is set to 70. Figure 4 shows the population transfer controlled by the pulse sequence produced by a OCT process. The final product yield is 97.3%. Although the pulse shape is different from that in the three-level π-pulse, i.e., there is only one node during irradiation of the laser pulse, the time evolution of the population is similar to that in the three-level π-pulse.

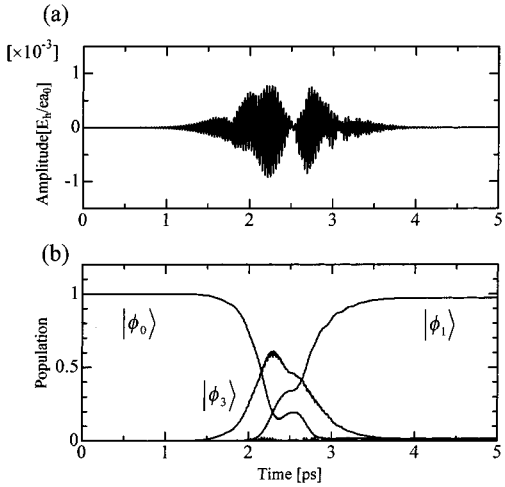

Figure 4. (a) Electric field designed by optimal control theory and (b) population dynamics. Initial electric field is given by two cw lasers, where laser frequencies are $\omega_1 = \omega_{30}$ and $\omega_2 = \omega_{31}$, and amplitudes are $E_1^0 = E_2^0 = 3.0 \times 10^{-4}\ E_h/ea_0$. Shape function $s(t)$ is given by a single Gaussian function with $\sigma = 0.76$ ps, and the penalty factor is 70.

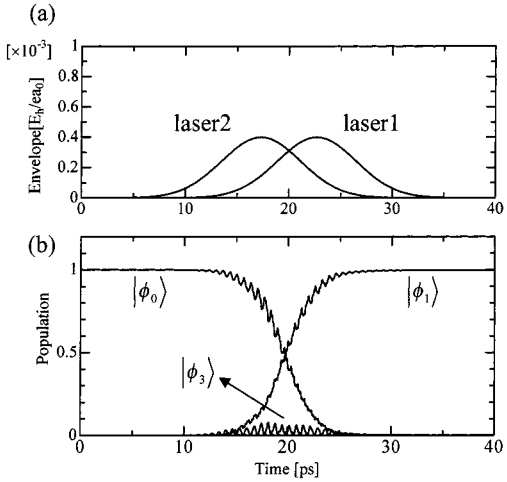

Figure 5. (a) Electric field of STIRAP and (b) population dynamics. Laser parameters are as follows: $E_1^0 = E_2^0 = 4.0 \times 10^{-4}\ E_h/ea_0$, $\sigma_1 = \sigma_2 = 5.4$ ps, and $t_2 - t_1 = -5.4$ ps.

5. STIRAP Technique

In this section, we present the results of simulation of proton transfer controlled by STIRAP. We consider the effective three-level system composed of $|\phi_0\rangle$, $|\phi_3\rangle$, and $|\phi_1\rangle$ coupled with two laser fields. Here, we use the same function as that used in the π-pulse approach for the electric field. Figure 5 shows a STIRAP pulse sequence and corresponding population dynamics. As seen in Figure 5a, the characteristics of STIRAP are (i) laser2 precedes laser1 unlike the order of two sequential π-pulses, (ii) two pulses have a large temporal overlap, and (iii) each pulse has a large pulse area. In our simulation, pulse area is set to 8π. Interestingly, the population moves from $|\phi_0\rangle$ to $|\phi_1\rangle$ without an appreciable population in the intermediate state $|\phi_3\rangle$. The mechanism of the population transfer is interpreted by the time

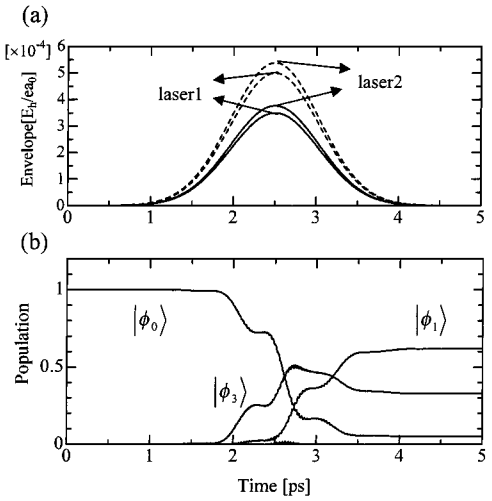

Figure 6. (a) Electric field of three-level π-pulse and (b) population dynamics. Laser parameters are as follows: $E_1^0 = 3.5 \times 10^{-4}$ E_h/ea_0, $E_1^0 = 3.8 \times 10^{-4}$ E_h/ea_0, $\sigma_1 = \sigma_2 = 2.2$ ps, and $t_2 - t_1 = 0$. Dashed lines are as in Figure 3.

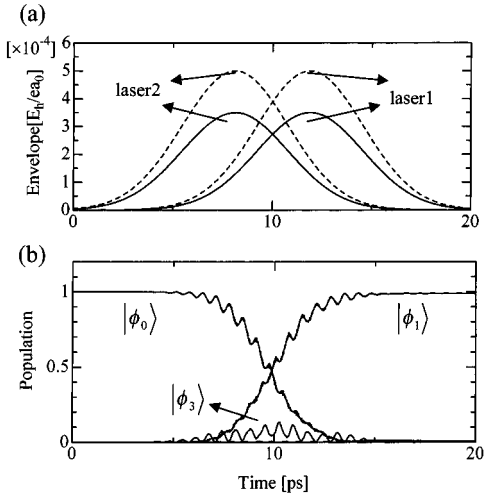

Figure 7. (a) Electric field of STIRAP and (b) population dynamics. Laser parameters are as follows: $E_1^0 = E_1^0 = 2.8 \times 10^{-4}$ E_h/ea_0, $\sigma_1 = \sigma_2 = 5.4$ ps, and $t_2 - t_1 = -5.4$ ps. Dashed lines are as in Figure 5.

evolution of one dressed state composed of $|\phi_0\rangle$, $|\phi_1\rangle$.[41] To show its robustness, we compared the population transfer of STIRAP with that of the three-level π-pulse by changing the pulse width and maximum amplitude. Figures 6 and 7 show the population dynamics of the three-level π-pulse and STIRAP when pulse intensities were decreased by 30%. The final product yield of the π-pulse approach is about 60%. In contrast, STIRAP keeps almost 100% of the product yield. When pulse widths are increased by 30%, similar results were obtained (not shown); i.e., the efficiencies of population transfer were about 60% and 100% for the π-pulse approach and STIRAP, respectively.

6. Chirped Laser Pulse

We have shown that STIRAP enables complete population transfer under very relaxed conditions of the laser parameters. However, the population-transfer process by STIRAP takes a relatively long time in comparison with that by the π-pulse approach, and effects of relaxation such as IVR on the efficiency of the population transfer may therefore be greater in the case of STIRAP than in the case of the π-pulse approach. To try to resolve this problem, we used a single infrared-domain chirped laser pulse. We show that a single chirped laser pulse with an

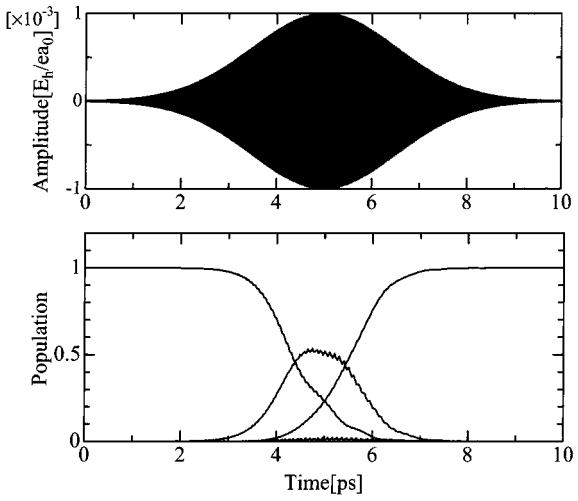

Figure 8. (a) Envelope of negatively chirped laser pulse and (b) population dynamics. Laser parameter are as follows: E^0 is 1.0×10^{-3} E_h/ea_0, $\sigma = 2.2$ ps, $c = 3.6$ cm^{-1}/fs.

appropriate chirping rate allows fast population transfer while maintaining robustness.

The electric field takes the following form:

$$E(t) = E^0 g(t) \cos \omega(t) \tag{29}$$

$$\omega(t) = \omega_0 t + \frac{1}{2} c(t - t_m)^2 \tag{30}$$

where E° is the maximum amplitude, $g(t)$ is the Gaussian function with width σ and time center t_m, ω_0 is the central frequency, and c is the frequency swept rate. When $c > 0$, it is called positive chirp, and $c < 0$ is negative chirp. We employ a single negative chirp for the control of proton transfer. We set the central frequency to $\omega_0 = (\omega_{30} + \omega_{31})/2$. This choice enables consecutive passage to two resonant frequencies, ω_{30} and ω_{31}, around the maximum of the envelope of the electric field.[62] Figure 8 shows the population transfer by negative chirp. Negative chirp moves the population from $|\phi_0\rangle$ to $|\phi_1\rangle$ via $|\phi_3\rangle$. The population transfer is achieved within about 4 ps. The results in the case of negative chirp are similar to those in the case of a three-level π-pulse or a pulse sequence designed by an OCT process. However, comparison of the product yields obtained with changes in the laser parameters shows that these properties are quite different. Figure 9 shows the final product yields of $|\phi_1\rangle$ with variation in the pulse area by changing pulse width in the case of (a) a three-level π-pulse and (b) negative chirp. In the case of π-pulse, the final product yield oscillates with change in the pulse area due to the Rabi frequency. In contrast, in the case of negative chirp, the efficiency of population transfer is low in the small pulse area. However, a very high product yield is maintained in the region of more than 5π.

7. Conclusion

We simulated the laser-induced intramolecular proton transfer by several approaches. The motion of a proton has been treated by asymmetric, one-dimensional double-well potential whose parameters ware chosen so as to describe the substituent effect such as $-NH_2$ and $-CH_3$ in malonaldehyde. In this model, the potential barrier is rather low, and there is therefore only one localized state in each well. We regarded one localized state as a reactant and the other as a product. The strategy to control the motion of a proton is to induce a transition from the reactant to the product by a laser pulse sequence. We first simulated

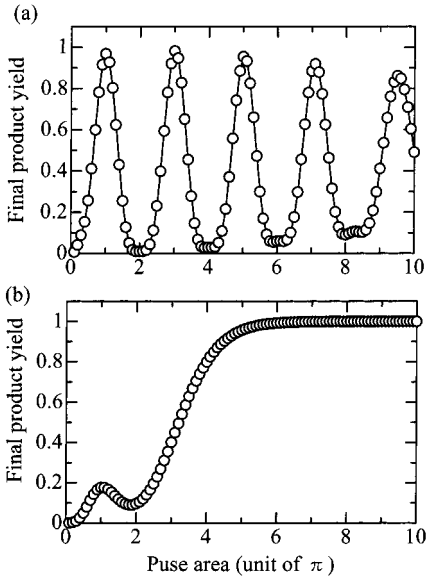

Figure 9. (a) Envelope of negatively chirped laser pulse and (b) population dynamics. Laser parameter are as follows: E^0 is 1.0×10^{-3} E_h/ea_0, $\sigma = 2.2$ ps, $c = 3.6$ cm^{-1}/fs.

the proton-transfer dynamics by using the π-pulse approaches, in which two IR laser pulses are sequentially or simultaneously applied to move the population from the reactant to the product. In the case of stepwise excitation by sequential irradiation of two pulses, the condition of population transfer to the target state is $\int dt\ \Omega(t)$ for each approximate two-level system coupled with one laser pulse. For simultaneous irradiation of two laser pulses, we gave the conditions of population transfer from the reactant to the product, and we called the pulse sequence satisfying this condition a three-level π-pulse. Next, we simulated proton transfer controlled by a pulse sequence designed by an OCT process in which the initial guess was set to a cw laser composed of two laser fields and single Gaussian function was chosen as a shape function. We have shown that the resultant population transfer is similar to that in the case of a three-level π pulse, although the pulse shapes in these two approaches seem to be rather different; i.e., the OCT pulse sequence looks like two sequential pulses. However, this may be due to interference between ω_{30} and ω_{31} components in the laser field.

We applied STIRAP and a negatively chirped laser pulse to the proton-transfer system to try to find a pulse sequence that gives a robust solution, and we found that these approaches enable effective population transfer under very relaxed conditions of laser parameters compared with π-pulse approaches.

The results showed that a negatively chirped laser pulse is particularly effective. The greatest advantage of this approach is that it may enable fast population transfer while maintaining robustness under very simple structure of the electric field. We have shown that the chirped laser pulse moves the population about 5 times faster than does STIRAP.

References and Notes

(1) Shi, S.; Woody, A. Rabitz, H. *J. Chem. Phys.* **1988**, *88*, 70.
(2) Shi, S.; Rabitz, H. *J. Chem. Phys.* **1990**, *92*, 2927.
(3) Shen, L.; Rabitz, H. *J. Chem. Phys.* **1994**, *100*, 4811.
(4) Zhu, W.; Rabitz, H. *J. Chem. Phys.* **1998**, *109*, 385.
(5) Zhu, W.; Botina, J.; Rabitz, H. *J. Chem. Phys.* **1998**, *108*, 1953.
(6) N. Došlić, Kühn, O.; Manz, J.; Sundermann, K. *J. Phys. Chem. A* **1998**, *102*, 9645.
(7) Malinovsky, V. S.; Tannor, D. J. *Phys. Rev. A* **1997**, *56*, 4929.
(8) Sola, I. R.; Malinovsky, V. S.; Tannor, D. J. *Phys. Rev. A* **1999**, *60*, No 4, 3081.
(9) Paramonov, G. K. In *Femtosecond Chemistry*; Manz, J., Wöste, L., Eds.; Verlag-Chemie: Weinheim, 1995; Vol. 2, pp 671−712.
(10) Korolkov, M. V.; Paramonov, G. K.; Schmidt, B. *J. Chem. Phys.* **1996**, *105*, 1862.
(11) Combariza, J. E.; Just, B.; Manz, J.; Paramonov, G. K. *J. Phys. Chem.* **1991**, *95*, 10351.
(12) Korolkov, M. V.; Paramonov, G. K.; Schmidt, B. *J. Chem. Phys.* **1996**, *105*, 1862.
(13) Combariza, J. E.; Just, B.; Manz, J.; Paramonov, G. K. *J. Phys. Chem.* **1991**, *95*, 10351.
(14) Korolkov, M. V.; Manz, J.; Paramonov, G. K. *Chem. Phys.* **1997**, *217*, 341.
(15) Korolkov, M. V.; Paramonov, G. K. *Phys. Rev.* **1997**, *A55*, 589.
(16) Korolkov, M. V.; Paramonov, G. K. *Phys. Rev.* **1997**, *A56*, 3860.
(17) Korolkov, M. V.; Paramonov, G. K. *Phys. Rev.* **1998**, *A57*, 4998.
(18) Gaubatz, U.; Rudecki, P.; Schiemann, S.; Bergmann, K. *J. Chem. Phys.* **1990**, *92*, 5363.
(19) He, G.; Kuhn, A.; Schiemann, S.; Bergmann, K. *J. Opt. Soc. Am.* **1990**, *B7*, 1960.
(20) Rubahn, H.-G.; Konz, E.; Schiemann, S.; Bergmann, K. *Z. Phys. D* **1991**, *22*, 401.
(21) Dittmann, P.; Pesl, F. P.; Martin, J.; Coulston, G. W.; He, G. Z.; Bergmann, K. *J. Chem. Phys.* **1992**, *97*, 9472.
(22) Schiemann, S.; Kuhn, A.; Steuerwald, S.; Bergmann, K. *Phys. Rev. Lett.* **1993**, *71*, 3637.
(23) Lawall, J.; Prentiss, M. *Phys. Rev. Lett.* **1994**, *72*, 993.
(24) Halfmann, T.; Bergmann, K. *J. Chem. Phys.* **1996**, *104*, 7068.
(25) Lindinger, A.; Verbeek, M.; Rubahn, H.-G. Z. *Phys. D* **1997**, *39*, 93.
(26) Oreg, J.; Hioe, F. T.; Eberly, J. H. *Phys. Rev.* **1984**, *A29*, 690.
(27) Gaubatz, U.; Rudecki, P.; Becker, M.; Schiemann, S.; Külz, M.; Bergmann, K. *Chem. Phys. Lett.* **1988**, *149*, 463.
(28) Kuklinski, J. R.; Gaubatz, U.; Hioe, F. T.; Bergmann, K. *Phys. Rev.* **1989**, *40*, 6741.
(29) Carroll, C. E.; Hioe, F. T. *J. Opt. Soc. Am.* **1988**, *B5*, 1335.
(30) Carroll, C. E.; Hioe, F. T. *Phys. Rev. A* **1990**, *42*, 1522.
(31) Shore, B. W.; Bergmann, K.; Oreg, J.; Rosenwaks, S. *Phys. Rev. A* **1991**, *44*, 7442.
(32) Band, Y. B.; Julienne, P. S. *J. Chem. Phys.* **1991**, *94*, 5291.
(33) Band, Y. B.; Julienne, P. S. *J. Chem. Phys.* **1992**, *96*, 3339.
(34) Band, Y. B.; Julienne, P. S. *J. Chem. Phys.* **1992**, *97*, 9107.
(35) Smith, A. V. *J. Opt. Soc. Am. B* **1992**, *9*, 1543.
(36) Band, Y. B.; Magnes, O. *J. Chem. Phys.* **1994**, *101*, 7528.
(37) Vitanov, N. V.; Stenholm, S. *Opt. Commun.* **1996**, *127*, 215.
(38) Vitanov, N. V.; Stenholm, S. *Phys. Rev.* **1997**, *A55*, 648.
(39) Kobrak, M. N.; Rice, S. A. *Phys. Rev.* **1998**, *A57*, 1158.
(40) Ohta, Y.; Kizu, H.; Yoshimoto, K.; Yamada, A.; Nishikawa, K. *Int. J. Quantum. Chem. Symp.* **1999**, *75*, 511.
(41) Ohta, Y.; Yoshimoto, T.; Nishikawa, K. *Chem. Phys. Lett.* **2000**, *316*, 551.
(42) Ohta, Y.; Yoshimoto, T.; Bando, T.; Nagao, H.; Nishikawa, K. *Int. J. Quantum. Chem. Symp.*, in press.
(43) Melinger, J. S.; Hariharan, A.; Gandhi, S. R.; Warren, W. S. *J. Chem. Phys.* **1991**, *95*, 2210.
(44) Melinger, J. S.; Gandhi, S. R.; Hariharan, A.; Tull, J. X.; Warren, W. S. *Phys. Rev. Lett.* **1992**, *68*, 2000.
(45) Broers, B.; Van Linden and van den Heuvell, H. B.; Noordam, L. D. *Phys. Rev. Lett.* **1992**, *69*, 2062.
(46) Melinger, J. S.; Gandhi, S. R.; Warren, W. S. *J. Chem. Phys.* **1994**, *101*, 6439.
(47) Kohler, B.; Krause, J. L.; Raksi, F.; Rose-Petruck, C.; Whitnell, R. M.; Wilson, K. R.; Yakovlev, V. V.; Yan, Y.; Mukamel, S. *J. Chem. Phys.* **1993**, *97*, 12602.
(48) Balling, P.; maas, D. J.; Noordam, L. D. *Phys. Rev.* **1994**, *A*50, 4276.
(49) Kohler, B.; Yakovlev, V. V.; Che, J.; Krause, J. L.; Messina, M.; Wilson, K. R.; Schwentner, N.; Whitnell, R. M.; Yan, Y. *Phys. Rev. Lett.* **1995**, *74*, 3360.
(50) Krause, J. L.; Messina, M.; Wilson, K. R.; Yan, Y. *J. Phys. Chem.* **1995**, *99*, 13736.
(51) Chelkowski, S.; Bandrauk, A. D.; Corkum, P. B. *Phys. Rev. Lett.* **1990**, *65*, 2355.
(52) Chelkowski, S.; Bandrauk, A. D. *J. Chem. Phys.* **1993**, *99*, 4279.
(53) Chelkowsi, S.; Gibson, G. N. *Phys. Rev.* **1995**, *A52*, 4317.
(54) Melinger, J. S.; McMorrow, D.; Hillegas, C.; Warren, W. S. *Phys. Rev.* **1995**, *A51*, 3366.
(55) Liu, W.-K.; Wu, B.; Yuan, J. M. *Phys. Rev. Lett.* **1995**, *75*, 1292.
(56) Mishima, K.; Yamashita, K. *J. Chem. Phys.* **1998**, *109*, 1801.
(57) Yuan, J. M.; Liu, W.-K. *Phys. Rev.* **1998**, *A57*, 1992.
(58) Meyer, S.; Meier, C.; Engel, V. *J. Chem. Phys.* **1998**, *108*, 7631.
(59) Yuan, J. M.; Liu, W.-K.; Hayashi, M. T.; Lin, S. H. *J. Chem. Phys.* **1999**, *110*, 3823.

(60) Kim, J.-H.; Liu, W.-K.; McCourt, F. R. W.; Yuan, J.-M. *J. Chem. Phys.* **2000**, *112*, 1757.
(61) Cao, J.; Bardeen, C. J.; Wilson, K. R. *J. Chem. Phys.* **2000**, *113*, 1898.
(62) Ohta, Y.; Bando, T.; Yoshimoto, T.; Nishi, K.; Nagao, H.; Nishikawa, K. *J. Phys. Chem.*, submitted for publication.
(63) Judson, R. S.; Rabitz, H. *Phys. Rev. Lett.* **1992**, *68*, 1500.
(64) Rabitz, H.; de Vivie-Riedle, R.; Motzkus, M.; Kompa, K. *Science* **2000**, *288*, 824.
(65) Assion, A.; Baumert, T.; Bergt, M.; Brixner, T.; Kiefer, B.; Seyfried, V.; Strehle, M.; Gerber, G. *Science* **1998**, *282*, 919.
(66) Marston, C. C.; Balint-Kurti, G. G. *J. Chem. Phys.* **1989**, *91*, 3571.
(67) Allen, L.; Eberly, J. H. *Optical Resonance and Two-Level Atoms*; Wiley: New York, 1975.